High-resolution imaging of a single circular surface acoustic wave source: Effects of crystal anisotropy

T. Hesjedal[a)]
Solid State and Photonics Lab, Stanford University, Stanford, California 94305

G. Behme
Paul Drude Institute for Solid State Electronics, Hausvogteiplatz 5-7, D-10117 Berlin, Germany

(Received 30 March 2001; accepted for publication 18 June 2001)

We present an experimental method for the high-resolution imaging of the excitation and propagation of surface acoustic waves (SAWs) on anisotropic piezoelectric substrates. By employing a scanning acoustic force microscope (SAFM), we are able to image acoustic waves that are excitable by a single circular electrode pair source through the mixing with well-defined reference plane waves. We show amplitude and phase images of the point-source wave field, containing the angular dependence of the phase velocity of these modes, as well as their electromechanical coupling strength. The SAFM allows easy access to acoustic material properties, which are important for the design of commercial SAW devices. © *2001 American Institute of Physics.* [DOI: 10.1063/1.1394170]

The propagation of acoustic waves in anisotropic materials is a complicated problem, mainly as group and phase velocity directions often differ from each other.[1,2] In this respect, wave excitation from point sources offer interesting physical insight into crystal properties, as special directions may exist in which acoustic energy is focused (phonon focusing).[3] Various methods have been successfully applied to the measurement of the surface wave slowness curve [the angular dependence of the inverse of the surface acoustic wave (SAW) phase velocity]. Several schemes rely on a point-source/point-receiver configuration, either employing a pulsed laser source and a mechanical point contact detector,[4] two point contact transducers,[5] or two acoustic lenses.[6] An all-optical scheme is, e.g., based on the scanning laser acoustic microscope.[7] A simple and robust technique is based on a broadband line-focus acoustic microscope.[8] In these ways, group and also phase velocities can be measured with great precision.

SAWs are widely used for modern filtering applications, mainly in communication devices. They are excited by interdigital transducers (IDTs) on the surface of a piezoelectric crystal. As the desired operation frequency range extends well beyond 2 GHz, the use of faster piezoelectric materials[9] or faster acoustic modes[10] becomes desirable. Especially since higher operation frequencies can be achieved without decreasing the lithographical feature sizes. Also, the use of materials with a high electromechanical coupling coefficient K^2, such as potassium niobate, offers a superior device performance through a low insertion loss.[11,12] For the design of advanced SAW devices, the wave fields have to be analyzed with high lateral resolution. Moreover, the acoustic energy conversion efficiency, expressed by the electromechanical coupling coefficient K^2, has to be measured.[13] By investigating an acoustic point source (e.g., a circular single finger IDT), the wave propagation in all piezoelectrically excitable directions can be studied simultaneously.

In this letter, we present the imaging of the angular dependence of SAW excitation (K^2) and propagation (phase velocity) from a circular *single* finger source on (001) GaAs with high lateral resolution using the scanning acoustic force microscope (SAFM). We show the utility and simplicity of this technique and suggest it could be of great use in a wide range of acoustic wave applications.

This experimental approach relies on the study of *single* acoustic sources, which are difficult to study by common SAW analysis methods. The scanning acoustic force microscope, on the other hand, is sensitive enough to study wave phenomena of *single* sources concerning both vertical sensitivity (sub 0.1 pm)[14] and lateral resolution (20 nm).[15] The SAFM is used to detect ultrasonic surface oscillations of arbitrary polarization with submicron lateral resolution.[16] It is based on an atomic force microscope (AFM) in contact mode and it utilizes the nonlinearity of the force-distance curve in the sense of a mechanical diode. Various ultrasonic force microscopes based on this principle have been developed in recent years.[17–20] The mechanical diode can be either used to demodulate an amplitude-modulated wave yielding its amplitude, or, to mix two slightly frequency-detuned waves (f_1, f_2) in order to access both phase and amplitude. The latter case leads to cantilever oscillations at the difference frequency of both waves ($\Delta f = f_1 - f_2$). Δf is chosen to be around the cantilever's resonance frequency f_{res}, or at its higher harmonics nf_{res}. The cantilever oscillation is conveniently measured using the AFM's conventional optical deflection technique. The deflection signal is then picked up by a lock-in amplifier and the obtained phase and amplitude signals are recorded simultaneously along with the topography signal.

Figure 1 shows a schematic of the experimental setup (based on an M5 AFM from ThermoMicroscopes; for experimental details see, e.g., Ref. 14). Typical scan frequencies range from 0.2 to 1 Hz. All presented data were obtained

a)Electronic mail: thorsten@snow.stanford.edu

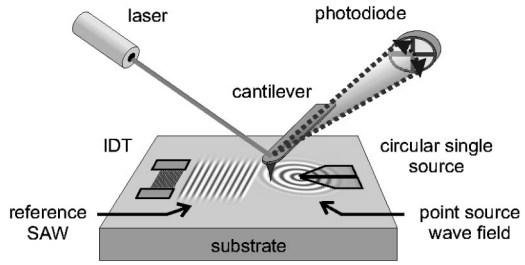

FIG. 1. Sketch of the SAFM experimental setup. The reference plane wave is launched towards the tip for sampling the complex radiation pattern of the single circular source.

using Si_3N_4 microlevers (ThermoMicroscopes). The circular single source is illuminated by a reference plane wave field coming from the left-hand side (SAW amplitude $A_{\mathrm{ref}} \approx 0.1\,\mathrm{nm}$). Common rf input powers fed to the transducers are $\geqslant 10\,\mathrm{dBm}$ (electrically unmatched).

In order to simulate the expected SAFM amplitude and phase contrast, we developed a simple model, which is described in detail elsewhere.[14] It is based on the approximation of the nonlinear force acting on the cantilever by a power series. Since the frequency of surface oscillations due to SAWs is of the order of typically 100 MHz to some GHz and the resonance frequency of the cantilever is of the order of some 10 kHz, it is reasonable to neglect all odd power terms (in the low-frequency limit). Then, the next nonvanishing term is the quadratic term $F \sim x_1 x_2$. When two SAWs $x_{1/2} = A_{1/2} \sin(\omega_{1/2} t)$ of different frequencies f_1 and f_2 are launched towards the tip, the force contains two components, one at the sum frequency $\Omega = \omega_1 + \omega_2$ and one at the difference frequency $\Delta\omega = \omega_1 - \omega_2$. The oscillation at Ω is averaged out, while the term at $\Delta\omega$ can be picked up by a lock-in amplifier delivering the cantilever signal S_{lever}.

For the general case of two propagating SAWs with wave vectors $\mathbf{k}_1$ and $\mathbf{k}_2$ (where in general $\mathbf{k}_1 \nparallel \mathbf{k}_2$), the cantilever signal becomes: $S_{\mathrm{lever}} = A(A_1, A_2) \cdot \sin[(\omega_1 - \omega_2)t + \mathbf{k}_1\mathbf{r}_1 - \mathbf{k}_2\mathbf{r}_2]$. The *expected* SAFM amplitude signal (at $\Delta\omega$) is independent of the position within an undisturbed wave field and depends only on both SAW amplitudes and the shape of the effective nonlinear force interaction.[15] It has to be pointed out that the amplitude contrast details in a given propagation direction are due to waves that are launched via electromagnetic crosstalk between the transducers and do not reflect the pristine amplitude distribution of the single source.[21] The SAFM phase, on the other hand, is determined by the difference of the contributing wave vectors $\Delta\mathbf{k}$. In case of $\mathbf{k}_1 \parallel \mathbf{k}_2$, the spatial evolution of the phase signal will be linear with a periodicty of half the wavelength $\lambda/2$ ($\lambda = 2\pi/k_1 \approx 2\pi/k_2$). It must be noted that this simple picture holds only for the case that exactly two waves contribute to the mixing signal. This is generally not true as, for instance, wave scattering leads to additional waves.

Figure 2 shows a simulation of SAFM amplitude (a) and phase (b) for the investigated experimental problem based on this model (including cross talk). We took a circular source on an isotropic substrate with angle-independent coupling factor into account. The reference wave was launched from the left-hand side. The phase output was restricted to a 2π range to make comparison with the measured phase easier (using a lock-in amplifier).

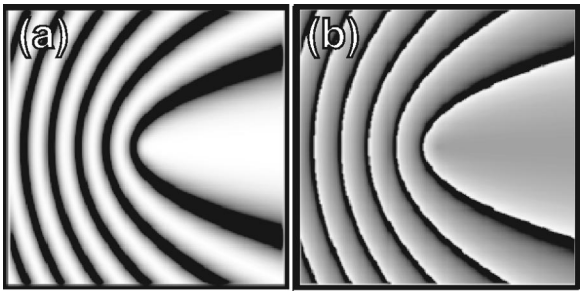

FIG. 2. Simulation of the SAFM amplitude (a) and phase (b) signal for the mixing of a plane wave with the wave field of an ideal circular source (without taking the substrate anisotropy or the electromechanical coupling strength into account).

The circular single SAW source under investigation was fabricated by electron beam lithography on (001) GaAs. The reference plane wave field was excited by a wide aperture split-finger IDT along a [110] direction at a frequency of 890 MHz ($\lambda = 3.2\,\mu\mathrm{m}$). The topography scan [Fig. 3(a)] shows the circular hot electrode (connected to rf phase), which is surrounded by a grounded ring electrode (connected to rf ground). The diameter of the inner circle is 4 μm, the gap is 1 μm wide, and the width of the outer ring is 2 μm. Thus, the excitable wavelength range is from 1 to 7 μm. This translates (at a fixed applied frequency of 890 MHz) to a covered phase velocity range from 890 to 6230 m/s where piezoelectrically excitable acoustic modes may be sampled.

The SAFM amplitude measurement [Fig. 3(b)] shows that directions parallel to and 90° off the reference propagation direction are preferred wave excitation directions. Most of the energy is radiated in a cruciform pattern defined by the crystalline directions with the highest electromechanical coupling coefficient. The behavior in the regions above and be-

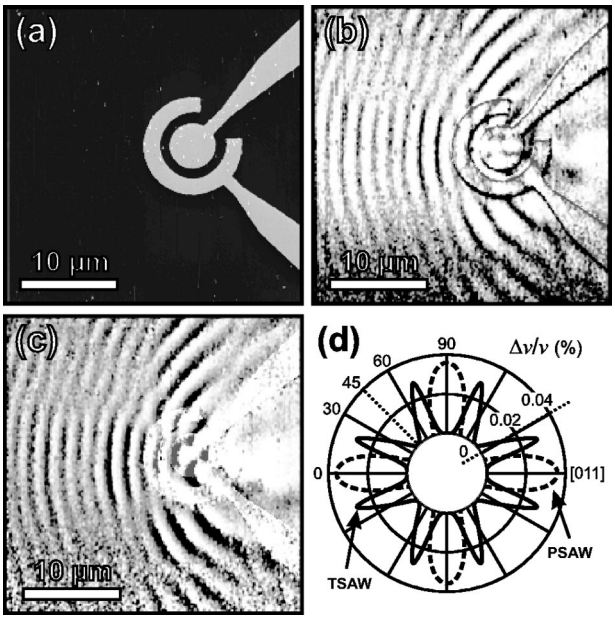

FIG. 3. Circular single source [Al electrodes, inner diameter: 4 μm, gap width: 1 μm, (001) GaAs]: (a) topography, (b) amplitude, and (c) phase image. The plane sample wave was launched from the left at 890 MHz ($\lambda = 3.2\,\mu\mathrm{m}$). The amplitude (b) and phase (c) images show the excited wave field with the preferred excitation directions. (d) Polar plot of the electromechanical coupling coefficient for the true SAW (TSAW) and the pseudo SAW (PSAW).

low the circle is due to equivalent waves propagating under an angle of 90° with respect to each other (see also Fig. 2). In the phase image (and also in the amplitude image), this leads to 45° tilted phase fronts [Fig. 3(c); compare to Fig. 2(b)]. Note that the angles used in Fig. 3(d) are not identical with the third Euler angles for these propagation directions, i.e., 45° for the [110] direction. Also, in the direction towards the reference IDT, waves are launched, which result in a periodicity of the phase discontinuities of $\lambda/2=1.6\,\mu$m. Conversely, the phase in the region behind the source is not modulated with a periodicity of $\lambda/2$, although a significant oscillation amplitude is present [Fig. 3(c)]. This is due to the wave vectors **k** of reference and excited SAW being parallel, thus their difference is very small leading to only negligible spatial rise of the phase signal. The wave field pattern obtained in the directions between 0° and 90° is complicated, because of the various effects of the anisotropy (phonon focusing, electromechanical coupling efficiency) of the cubic substrate.[22] As already mentioned, a Rayleigh wave is found in the 45° direction that shows no electromechanical coupling [Fig. 3(d); true SAW (TSAW)]. In-between 0° and 45°, a coupling pseudo SAW mode is found at roughly 23° that shows vanishing beam steering [Fig. 3(d); PSAW]. Around 23° and 0°, wave modes are excited that show high damping and a large beam-steering effect for deviating propagation angles. However, the energy flux is concentrated in the 0° and 90° directions. The observed phase pattern within the ring transducer will be subject to further investigations.

In this letter, we present the high-resolution imaging of SAW excitation and propagation from a circular single source on GaAs using a SAFM mixing technique. From the amplitude and phase images, the angular dispersion of SAW slowness of all excitable modes, as well as the electromechanical coupling coefficient, can, in principle, be extracted. Measurements like these will be of great importance for evaluating the acoustic properties of novel material systems for the application in SAW devices. Also, it opens a way for the study of material anisotropy on the nanoscale. Future work will focus on the solving of the inverse problem of extracting numerical values for the phase velocities and coupling constants.

The authors thank C. F. Quate for help and discussions, and G. S. Solomon for proofreading the manuscript. Supported by the DFG.

[1] B. A. Auld, *Acoustic Fields and Waves in Solids* (Wiley, New York, 1973).
[2] G. S. Kino, *Acoustic Waves: Devices, Imaging, and Analog Signal Processing* (Prentice-Hall, Englewood Cliffs, NJ 1987).
[3] R. E. Vines, S. Tamura, and J. P. Wolfe, Phys. Rev. Lett. **74**, 2729 (1995).
[4] B. Castagnede, K. Y. King, W. Sachse, and M. O. Thompson, J. Appl. Phys. **70**, 150 (1991).
[5] J. P. Wolfe, Phys. Today **48**, 34 (1995).
[6] M. Pluta, M. Schubert, J. Jahny, and W. Grill, Ultrasonics **38**, 232 (2000).
[7] W. P. Robbins and E. P. Rudd, J. Appl. Phys. **64**, 1040 (1988).
[8] D. Xiang, N. N. Hsu, and G. V. Blessing, Appl. Phys. Lett. **74**, 2236 (1999).
[9] S. Shikata, H. Nakahata, A. Hachigo, and N. Fujimori, Diamond Relat. Mater. **2**, 1197 (1993).
[10] M. P. daCunha and E. L. Adler, IEEE Trans. Ultrason. Ferroelectr. Freq. Control **42**, 840 (1995).
[11] K. Yamanouchi and H. Odagawa, IEEE Trans. Ultrason. Ferroelectr. Freq. Control **46**, 700 (1999).
[12] V. G. Mozhaev and M. Weihnacht, Ultrasonics **37**, 687 (2000).
[13] K^2 is defined as $2\Delta v/v$, where Δv denotes the difference of the open-circuited and the short-circuited SAW phase velocity.
[14] T. Hesjedal and G. Behme, Europhys. Lett. **54**, 154 (2001).
[15] E. Chilla, T. Hesjedal, and H.-J. Fröhlich, Phys. Rev. B **55**, 15852 (1997).
[16] G. Behme and T. Hesjedal, Appl. Phys. Lett. **77**, 759 (2000).
[17] W. Rohrbeck and E. Chilla, Phys. Status Solidi A **131**, 69 (1992).
[18] O. Kolosov and K. Yamanaka, Jpn. J. Appl. Phys., Part 2 **32**, 1093 (1994).
[19] U. Rabe and W. Arnold, Appl. Phys. Lett. **64**, 1493 (1994).
[20] N. A. Burnham, A. J. Kulik, G. Gremaud, P. J. Gallo, and F. Oulevey, J. Vac. Sci. Technol. B **14**, 794 (1996).
[21] T. Hesjedal and G. Behme, IEEE Trans. Ultrason. Ferroelectr. Freq. Control **48**, 641 (2001).
[22] S. Tamura and M. Yagi, Phys. Rev. B **49**, 17378 (1994).